ASSESSMENT OF AEROACOUSTIC OPTIMISATION SCHEMES FOR A TILT-PROPELLER APPLICATION IN HOVER AND CRUISE

Ole Bergmann, FH Aachen, Aachen, Germany
Felix Möhren, FH Aachen, Aachen, Germany
David Frey, FH Aachen, Aachen, Germany
Frank Janser, FH Aachen, Aachen, Germany
Carsten Braun, FH Aachen, Aachen, Germany

Abstract

Balancing propeller optimisation between cruise and hover conditions is a key challenge in eco-friendly aircraft design. This paper presents a novel multidisciplinary propeller optimisation approach, integrating blade element momentum theory and acoustic models. Three propeller design strategies are systematically evaluated in multidisciplinary propeller optimisation, considering aerodynamic efficiency and noise emissions. The design strategies and the optimisation scheme are assessed within the paper. A serial optimisation scheme improves the overall optimisation result and reduces the optimisation time significantly. In the serial approach, the design space is reduced stepwise. In the initial step, linear chord and parabolic twist distributions are sufficient for defining global propeller parameters like blade number and diameter. In contrast, detailed blade shape optimisation requires a parametric blade description. The findings are utilized to develop a novel optimisation scheme, reducing computational effort and enabling innovative air mobility solutions to be designed.

1. NOTATION

Acronyms

AoA	Angle of Attack
BET	Blade Element Theory
BSO	Blade Shape Optimisation
CST	Class Shape Transformation
DS	Design Strategy
GPPO	Global Propeller Parameter Optimisation
MDO	Multidisciplinary Optimisation
SPL	Sound Pressure Level
UAM	Urban Air Mobility

Latin

a_a	Axial induction factor
A_{Prop}	Propeller area
a_t	Tangential induction factor
C_{chord}	Chord length
$c_{d_{alpha}}$	Drag coefficient as a function of angle of attack
F_{PTL}	Prandtl tip loss function
L_p	Sound pressure level
N_b	Blade number
T	Thrust
u	Circumferential velocity due to rotation
v_∞	Flight velocity
w	Absolut velocity
w_a	Axial-induced velocity
w_t	Tangential-induced velocity
X	Weighting function
x_W	Weighting exponent energy consumption
x_{SPL}	Weighting exponent noise emission

Greek

η	Efficiency
Γ	Circulation
$\omega_{Propeller}$	Angular velocity
ϕ	Helix angle
θ	Twist
ρ	Density
σ	Blade solidity

Subscripts

r	Local radius dependency
opt	Optimal blade section parameter

2. INTRODUCTION

Different manufacturers are developing various urban air mobility (UAM) concepts. Most concepts have in common that they use electrically driven propellers for propulsion and often for vertical take-off and landing. A wide variety of aircraft concepts with variable propulsion approaches are developed. Designing highly efficient propellers for these concepts is crucial for the aircraft concept's success.

One major challenge of urban air mobility is noise emissions for societal acceptance [1]. Therefore, the noise emissions of the UAM have to be as low as possible, while the propulsive efficiency has to be as high as possible. The primary noise sources of these concepts are the propellers, independent of the aircraft configuration. That is why propeller noise reduction is of great interest to researchers and manufacturers.

Optimisation of a propeller for a singular optimisation point according to the minimum induced loss (MIL) condition defined by Betz [2] is standard practice [3–5]. However, this procedure is valid for a single operating point, not a flight mission, and does not include noise emissions. Therefore, the current research uses multidisciplinary optimisation (MDO) to reduce noise emissions and maximize propeller efficiency for a mission.

Propeller optimisation is a multidisciplinary task that cannot be solved with a singular approach. Different tools with different levels of physical insights are used, depending on the design stage of the optimisation [6]. In the preliminary design, where the overall propeller geometry is defined, reduced-order models like the blade element momentum theory (BEMT) are used for the aerodynamic performance prediction. The BEMT has high accuracy with minimal calculation effort [7]. When optimising a propeller, at least aerodynamics and aeroelasticity should be considered [8–10]. The structure is generally modelled in the preliminary design with a beam theory. An efficient possibility to consider elasticity in an optimisation approach is a pre-deflection analysis, which is used to define the jig-shape of the propeller [11]. The authors presented the pre-deflection analysis's applicability for considering the elasticity in the propeller design in Ref. [11, 12]. The advantage of a jig-shape approach is the decoupling of the aerodynamic and structural optimisation problem. The aerodynamic optimisation can be performed without coupling to the structural simulation, which reduces the simulation effort. The jig-shape approach is performed after the aerodynamic optimisation.

However, static and dynamic strength at hover and forward flight have to be checked in an optimisation framework for complex propeller geometries with sweep and lean to avoid unfeasible designs. Consequently, at least the final design step of the optimisation should include coupled aeroelastic and acoustic calculations [13].

In the first step, the noise emission of a propeller can be estimated with derivations of the Ffowcs-Williams and Hawkings method for rotating geometries, according to Hanson [14] or Farassat [15]. Furthermore, the drive train can be considered for matching the propeller power consumption with the motor efficiency map [16, 17]. Finally, integrating the propeller into the aircraft concept could be considered. The aerodynamic interferences between propeller and aircraft surfaces or between different propellers are complex and influence the aircraft's overall performance and noise emissions. However, to capture this interference, the aircraft and the propeller's aerodynamics must be modelled with an appropriate approach capable of capturing this interference. Therefore, the aerodynamic propeller-interference is usually analysed in a second step, with a method that provides more physical insights, e.g., a potential panel solver. Such aspects are outside the scope of this paper.

The complexity of the optimisation problem with the high number of design variables, such as

1. Pitch setting
2. Diameter
3. Blade numbers
4. Chord distribution
5. Twist distribution
6. Sweep distribution
7. Lean distribution
8. Airfoil distribution
9. Root design
10. Tip design

requires an appropriate optimisation scheme, which cannot be derived from the literature. With the available computational power and high-performance computing clusters, the problem can be solved holistically in a single optimisation with all considerations. However, coupled aeroelastic and aeroacoustic simulations of the propeller are still time-consuming, which is why a breakdown of the optimisation problem in different steps might be helpful [13].

The aim of this paper is the comparison of different optimisation schemes to provide a novel guideline for the application of an optimisation scheme for propellers. A novel optimisation routine is presented and evaluated. A tilt propeller for hover, transition and cruise is designed for demonstration. These design points require different twist and chord distributions

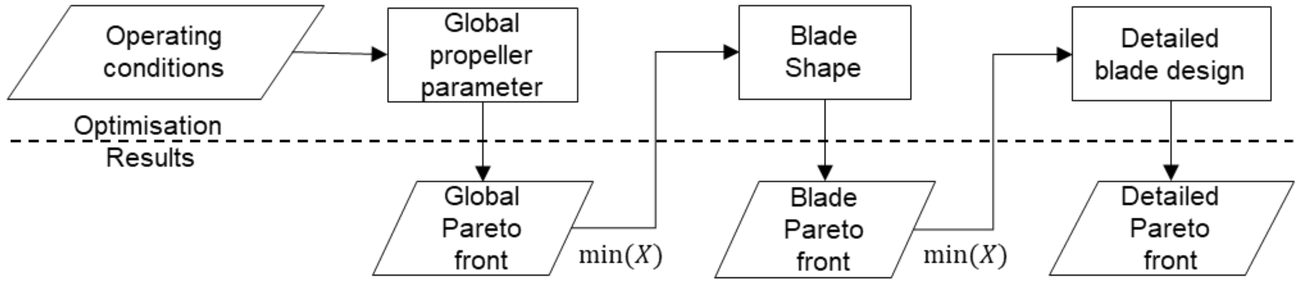

Figure 1 Flow chart of the optimisation process

and have contrary design goals. Consequently, numerical optimisation is necessary to find the optimum. Not all later stated steps can be performed and evaluated in this paper. The main focus is global and blade shape optimisation (GPPO / BSO), as the following paragraphs define.

3. NUMERICAL OPTIMISATION APPROACH

Different numerical optimisation schemes are used in literature for propeller optimisation. The genetic algorithm (GA) can be paralyzed and is capable of multi-objective design, which is required to find the Pareto-front between noise emissions and energy consumption [18, 19]. Additionally, the GA does not require differentiation, which is not available for discrete values like the number of propellers or blades.

Matlab offers various optimisation schemes, such as the GA, commonly used for propeller optimisation. The authors develop an optimisation scheme that increases fidelity and calculation effort in three steps presented in Figure 1 and Table 1. In each step, MDO calculates a Pareto front. The minimum weighting function X (presented later in eq. (1)) defines the inputs for the next optimisation step. All optimisation steps consider primary aeroelastic and aeroacoustic constraints listed below:

1. The blade tip Mach number has to be smaller than 0.75 to avoid shock waves
2. The aspect ratio of the blade should be higher than 6 to maintain the underlying assumptions of BEMT
3. The root chord length should be smaller than 20% of the diameter for realistic geometries
4. The tip chord-to-root ratio (taper ratio) should be between 0.2 and 1.

At first, the global propeller parameters listed in Table 1 are optimised. In this design stage, aircraft parameters are considered to find an appropriate propeller and reduce the parameter space for blade shape optimisation. The chord, twist and sweep distribution are optimised in the second step. In the final step, details of the blade are optimised under aeroacoustic and aeroelastic considerations. The following table shows the three optimisation steps' target parameters and the considered disciplines.

Table 1 Target optimisation parameters

Global parameter	Blade Shape	Detailed Blade Design
Diameter Blade number Pitch system	Twist dist. Chord dist. Sweep dist.	Lean dist. Airfoil dist. Tip design Root design
Aeroacoustic optimisation	Aeroacoustic optimisation	Aeroacoustic & aeroelastic optimisation

The numerical method is briefly described before explaining the optimisation scheme in detail.

3.1. Numerical Method

For the coupled calculation, the Matlab-based validated tool PropCODE is used. PropCODE uses an advanced BEMT solver for aerodynamic prediction. The BEMT solver combines XFOIL with a post-stall model for the 2D airfoil database. The general momentum theory is used for the prediction of thrust and torque. The BEMT is extended for swept propellers with a novel correction method [7, 20].

The noise emissions can be predicted with different noise models. An empirical category 1 model, according to Gutin [21, 22], or a physical bases category 2 method, according to Hanson [23] or Farassat [15], can be used within the optimisation. However, this paper is limited to using Farassat's formulation 1A according to the implementation in NASA's Aircraft Noise Prediction Program 2 (ANOPP2) [24]. The structural mechanics are modelled with a one-dimensional Timoshenko beam theory described in Ref. [9]. The aerodynamic forces described at the quarter chord axis are projected on the elastic axis for the aeroelastic calculations. The propeller geometry is described using the class function shape function transformation method (CST) according to Ref. [25]. The CST describes the geometry with a few polynomials for the twist, chord length, lean, sweep and airfoil sections. Depending on the geometric complexity, different orders of polynomials are required.

Further, the CST description allows to manipulate the geometry by simple changes of the splines. Therefore, this description can be used in optimisation. One of the later stated design strategies (DS) uses this formulation.

Within the MDO, three basic steps are performed.

1. A blade geometry is created
2. The aerodynamic performance of the geometry for the mission is analysed
3. The noise emissions are predicted

At first, a propeller geometry is designed. Second, the geometry is analysed in all optimisation steps to see if it fulfils the mission requirements. The mission analysis is used to calculate the energy consumption of the mission. The calculation of the energy consumption can be extended by considering a motor and pitch system model.

The energy consumption of a mission is a well-suited measure of propeller efficiency because it allows coupling multiple operating conditions with the durations of each operating point. Therefore, the aerodynamic efficiency can be reduced for various design points to one variable by summing the time-weighted power consumptions at the separate operating points.

In the case of a pitch system, the power consumption calculation has to be performed for different pitch angles. The minimal power consumption of the different pitch angles for a given operating point is searched.

If a motor should be considered, the propeller torque and rotational speed determine the motor efficiency at each operating point. The motor efficiency calculates the electric power consumption, which is then minimized.

Third, the noise emissions at a specific observer position and operating point are analysed.

A weighting function is required to balance energy consumption and noise emission. The weighting function X is defined as the multiplication of sound pressure level [dB] (SPL) and the energy consumption W [kWs]. Both factors are weighted to change the relevance of either the energy consumption or the noise emissions by the weighting exponents x_W and x_{SPL}. In the current study $x_W = 8$ and $x_{SPL} = 0.5$ are chosen. The exponents have been determined heuristically. The minimal weighting function defines the sweet spot of the Pareto front.

(1) $$X = W^{x_W} \cdot SPL^{x_{SPL}}$$

A weighting between these conditions is required if multiple noise operating points are considered. This acoustic weighting can be performed by a logarithmic sum of the sound pressure levels L_p.

(2) $$\mathrm{L}_{\mathrm{p},\Sigma} = 10 \log\left(\sum_{i=1}^{n} 10^{\frac{\mathrm{L}_{\mathrm{p,i}}}{10}}\right) dB$$

The analysis of the flight mission is reduced to three rotational speeds per operating point, fitted with a quadratic curve. The quadratic fit defines the rotational speed that matches the design thrust. This rotational speed is recalculated to determine the power consumption of the propeller at the design point. This procedure has to be repeated if the recalculated thrust does not match the design thrust.

The presented aerodynamic, acoustic and structural models fulfil the requirements of an MDO to be sufficiently accurate and computationally highly efficient.

3.2. Propeller Design in Optimisation

The authors identified three design strategies (DS) to find an appropriate geometry. Two are based on the definition of an ideally twisted propeller according to the MIL condition for a single operating point. The design operating point is varied to find a global minimum for the energy consumption of the mission. The third DS is based on an arbitrary chord and twist distribution definition. The three DS are used to design a propeller blade which is afterwards used to analyse the fight mission.

After the geometry design, the propeller is checked to fulfil basic assumptions for the calculation, e.g. the blades aspect ratio, which must be high enough to avoid violating the limits of the BEMT.

Design Strategy 1 (DS 1):

The geometry is designed for one operating point, consisting of a prescribed thrust (T), rotational speed, flight velocity (v_∞), number of blades (N_b) and diameter (D). It's known from the derivation of the MIL condition that the axial-induced velocity (w_a) across the propeller plane should be constant. As stated in eq (3), this induced velocity can be calculated with the momentum theory. This induced velocity is manipulated by the Prandtl tip loss factor F_{PTL}, derived in Ref. [2] to account for losses due to recirculation at the blade tip and vortices at the root (eq. 4).

To match the thrust requirement of the design point, the chord distribution (c_r) must be calculated according to eq. (5). However, in a standard MIL approach, the calculation of the chord distribution has to be iterated during the design of the propeller. This iteration is avoided by a variation of linear chord distributions used to calculate the propeller's thrust. The thrust calculation can be performed as a matrix multiplication which is much faster than an iterative scheme. The root chord length and the taper ratio describe the linear chord distributions. The chord distribution with the lowest thrust derivation to the design thrust is selected for the final geometry.

The twist distribution (θ) is constructed from the helix angle (ϕ) (eq. (6)) and the optimal angle of attack (α_{opt}) of the airfoils (see eq. (8)).

(3) $$\mathrm{w_a} = -\frac{\mathrm{v_\infty}}{2} \pm \sqrt{\left(\frac{\mathrm{v_\infty}}{2}\right)^2 + \frac{\mathrm{T}}{2\cdot\rho\cdot\mathrm{A_{Prop}}}}$$

(4) $$w_a = w_a \cdot F_{PTL}$$

(5) $$\frac{T}{N_b} = \int_{Root}^{Tip} \frac{\rho}{2} w^2 c_{l_{opt}} c_r \cos(\phi) dr$$

(6) $$\tan(\phi) = \frac{v_\infty + w_a}{u}$$

(7) $$w = \sqrt{u^2 + (v_\infty^2 + w_a^2)}$$

(8) $$\theta = \phi + \alpha_{opt}$$

The geometry can be designed without any iteration.

For DS 1, **five** optimisation parameters must be analysed independently of the pitch system. The optimisation parameters are design thrust, velocity, rotational speed, diameter, and blade numbers.

The advantage of the DS 1 is its minimal calculation time because it does not require any iterations. The disadvantage of DS 1 is that the propeller geometries are limited to a linear chord length distribution. Therefore, DS 1 can only be used to define the global propeller parameters like number of blades and diameter.

Design Strategy 2 (DS 2):

The above-stated procedure does not include airfoil drag, tangential-induced velocities, and a variation of axial-induced velocities. They can be included by an iterative scheme based on the general momentum theory as stated in eq. (9) - (14). An iterative scheme optimises twist and chord distribution for a single design point. However, the chord distribution is manipulated to match the optimal induced velocity and twist distribution.

(9) $$\mathrm{w_a} = \mathrm{v_\infty} \cdot \mathrm{a_a}$$

(10) $$\mathrm{a_a} = \frac{(1+\mathrm{a_a})\cdot\sigma\cdot[c_{l_{opt}}\cos(\phi) - c_{d_{opt}}\sin(\phi)]}{4\sin^2(\phi)}$$

(11) $$\mathrm{w_t} = \mathrm{u} \cdot \mathrm{a_t}$$

(12) $$\mathrm{a_t} = \frac{(1+\mathrm{a_t})\cdot\sigma\cdot[c_{l_{opt}}\sin(\phi) + c_{d_{opt}}\cos(\phi)]}{4\sin^2(\phi)} \cdot \frac{\mathrm{v_\infty}}{\mathrm{u}}$$

(13) $$\tan(\phi) = \frac{v_\infty + w_a}{u - w_t}$$

(14) $$w = \sqrt{(u - w_t)^2 + (v_\infty^2 + w_a^2)}$$

(15) $$\sigma = \frac{N_b \cdot c_r}{2\pi \cdot r_r}$$

σ is the solidity of the blade, a measure for the chord length of a blade section to the belonging circumference. Due to the iterative design scheme, DS 2 is more time-consuming than DS 1 and DS 3, but the aerodynamic design is optimal for a given design point, which is not valid for DS 1. Differently from DS 1, an initial guess of chord length and taper ratio is required. Therefore, **seven** parameters have to be optimised.

Design Strategy 3 (DS 3):

The blade design in DS 3 is based on the CST description. This DS does not include any aerodynamic consideration in the design of the propeller. An arbitrary blade geometry is designed and evaluated in the mission analysis whether the propeller meets the mission requirements or not.

A polynomial of fifth order describes the chord and twist distribution. Additionally, the diameter and the number of blades must be varied, resulting in **fourteen** parameters for DS 3. The CST parameters are initialised with a decreasing twist distribution from the hub to the tip and a decreasing chord length distribution to the tip.

After initialisation, the blade form can have an arbitrary shape between the tip and root. The global design space limits the root and tip variables.

The advantage of DS 3 is that the blade can have arbitrary twist and chord distributions. The propeller construction is a simple function evaluation, so it is much faster than DS 1 and 2. The advantage that the blade can have an arbitrary form is also a significant disadvantage because many designed geometries do not have the required blade forms to generate enough thrust. Therefore, a lot more function evaluations are required.

3.3. Optimisation Scheme

The optimisation should be performed in a serial approach, where the design space is stepwise reduced, and the simulation fidelity increases. Thereby, the convergence should be accelerated. In the following subchapters, the three optimisation steps are presented.

3.3.1. Global Propeller Parameter Optimisation

The global propeller parameter optimisation (GPPO) aims to define the diameter and number of blades for a given aircraft. The aircraft has thrust requirements at different operating conditions. These thrust requirements have to be fulfilled by the propulsion system. For example, a few aircraft concepts use some of their propellers for vertical take-off and landing and some propellers as tilt-propellers for vertical take-off and cruise (Hyundai, Archer Aviation, Vertical Aerospace). However, the number of propellers depends on the available space and the diameter of the propellers. Therefore, the optimal diameter and number of blades have to be identified. Finally, the decision for a variable pitch system or a fixed pitch propeller has to be made.

In this stage, the airfoil distribution is prescribed by the design engineer. The GPPO stage defines the diameter, number of blades, and suitable twist and chord parameters. The output of the GPPO is used in the BSO. The airfoil distribution selection is less critical than the aerodynamic performance [7, 26]. However, the thickness distribution might impact the propeller's noise emissions and static strength.

3.3.2. Blade Shape Optimisation

The blade shape optimisation (BSO) optimises the blade form. Diameter, number of blades, maximal and minimal root twist and chord, and taper ratio are prescribed by the GPPO. While blade diameter and number are fixed by the GPPO, the design space of twist and chord is only reduced to a smaller region. Consequently, the parameter space is drastically reduced. The geometry should be manipulated arbitrarily, which can only be achieved with DS 3. The optimal blade shape should be defined. In the BSO, propeller sweep can be used as an additional design variable.

If no further optimisation should be performed, a pre-deflection analysis generates the jig shape of the propeller.

3.3.3. Detailed Blade Design

This subsection describes the final step in optimising the blade shape. However, the detailed design is beyond the scope of this work as the complexity increases drastically. The increase in complexity is described below.

Depending on the design stage of the aircraft and application, a final optimisation can be performed. In the detailed blade design, the geometry is manipulated via the CST. In this final step, a closely coupled aeroelastic and aeroacoustic simulation should be performed to consider all relevant effects. However, this significantly increases the computational time because each propeller geometry must determine the structural cross-sectional parameters. The aerodynamic cross-sectional parameters do not change as long as the airfoil shape is not altered and sweep and lean are moderate. The structural simulation constrains the planform in high loading and high rotational speed conditions.

In this design stage, lean and sweep are optimised for the twist and chord distribution. The sweep and lean optimisation can only be done if aeroelasticity is considered. Due to the geometry's increased complexity, the polynomial order must be increased. The authors recommend using at least a sixth-order polynomial to discretise the radial geometry parameters. This results in **28** parameters for twist, chord, lean and sweep, which must be optimised. The airfoil's discretisation must be done with at least fourth-order polynomials for the upper and lower side of the airfoil. This polynomial leads to a minimal ten parameters per airfoil, with at least four blade stations per propeller to additionally **40** parameters. However, manipulating the airfoil requires additional calculations with XFOIL to generate the 2D aerodynamic data, significantly increasing the calculational effort. Therefore, this step should be obviated. Instead, the airfoils should be selected from a database, based upon the simulation results of the BSO.

As already stated, the detailed blade design is out of the scope of this paper because the overall DS is evaluated; therefore, the third design step is not required.

3.3.4. Hypotheses

The authors claim two hypotheses for the DS of the propeller. These hypotheses are verified in the following chapter on an example.

1. The GPPO stage requires only a reduced fidelity compared to the blade shape optimisation because detailed planform parameters should not be determined. Therefore, DS 1 should be used in the GPPO.
2. The serial optimisation scheme with GPPO and BSO is more efficient and robust than a single optimisation of all possible parameters.

4. ASSESSMENT OF THE DESIGN APPROACH

The assessment is performed through an example, where the mission parameters are presented in the table below. The noise emissions are optimised in hover conditions. The assessment is performed on MSL conditions, and the acoustic optimisation is performed at a reference distance of 300m.

As currently seen in tilt propeller applications, variable pitch systems are applied to reduce the conflict between hover and cruise condition. Therefore, the assessment is performed with a pitch system. The propeller can be pitched from -6 ° to 6 °.

Table 2 Design parameter

Design Point	Thrust [N]	Velocity [m/s]	Duration [min]
Cruise	300	30	48
Transition	600	15	12
Hover	1200	1	6

The geometry is constrained according to the following table:

Table 3 Geometric constraints

Constrains		Min	Max
Blades	[-]	3	9
Diameter	[m]	1.5	4
Taper ratio	[%]	20	100
Root chord length	[%]	5	30
Root twist	[deg]	15	75
Tip twist	[deg]	0	40
Sweep	[%]	0	20

Root chord length and sweep are normalized with the propeller diameter. The sweep is defined as a tangential tip displacement.

4.1. Assessment of the Design Strategies

In the first step, the first hypothesis is analysed. The DS is evaluated by performing the GPPO. The noise emissions are predicted with Farassat's formulation 1A because this solver has the highest fidelity.

In theory, DS 3 should find the propeller with the best ratio between noise emissions and power consumption. In practice, this is not the case due to the parameter space's complexity and the peculiarities of the geometry, which hinder the identification of a global minimum.

Figure 2 shows the Pareto fronts of the three DS. The markers in the figure represent the sweet spot in the Pareto front. The Pareto front with the lowest energy consumption results from DS 1. DS 2 and DS 3 do not reach the energy consumption of DS 1 in the given population size and number of generations. The lowest SPL results from DS 1 in the sweet spot. Concluding, for the given population size and number of generations, DS 1 leads to the best results. Therefore, it is used for comparison.

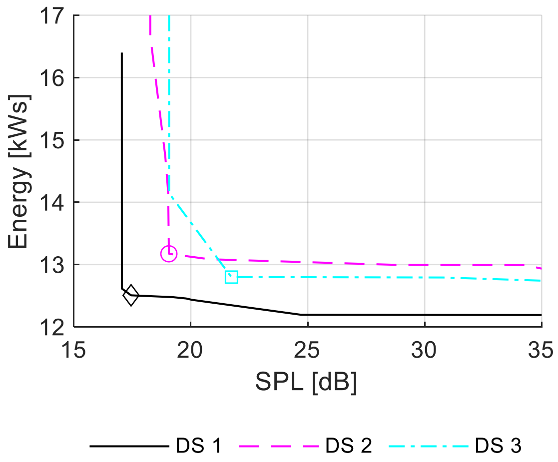

Figure 2 Global parameter Pareto fronts of different design strategies

The following table summarises the sweet spot results of DS 1, 2 and 3. The table shows the required simulation time and the parameters of the sweet spot. The table shows that all three DS lead to different diameters. The sweet spot of DS 1 leads to the best propeller for the mission with the lowest energy consumption and SPL. The energy consumption is 0.7 kWs lower and 4.3 dB quieter than the Pareto front of DS 3. DS 1 requires the least time for optimisation, whereas DS 3 takes roughly four times as much time.

The table shows that DS 3 does not lead to the same diameters as DS 1, and DS 2 does not lead to the same blade number. Both should be the same as DS 1 because DS 1 finds the best propeller. Therefore, DS 2 and 3 should not be used in the GPPO stage. The fast and robust DS 1 is preferred in the GPPO stage.

Table 4 Optimisation sweet spots

Design stategy		1	2	3
Simulation time	[h]	2.5	3.2	10.2
Energy consumption	[kWs]	12.5	13.2	12.8
Sound pressure level	[dB]	17.5	19.1	21.7
Blades	[-]	8	6	8
Diameter	[m]	3.66	3.66	2.86

Figure 3 presents the chord length and twist distribution of the sweet spots. The chord distribution differs between all three methods. DS 1 has a linear chord length resulting from the constraints of the design methods. The chord length distribution of DS 2 leads to a quadratic chord length behaviour due to the MIL condition. The blade shape of DS 2 is typically not built by propeller manufacturers because such root chord lengths are difficult to manufacture. DS 3 can have an arbitrary chord length distribution. The shown distribution is a typical blade shape known from acoustic optimisation studies [27, 28].

The twist distribution is similar in all three methods, which shows that the approach of DS 1 works. That the twist distributions are similar was expected. They are defined by the velocity field, which is the same independent of the DS and chord length distribution.

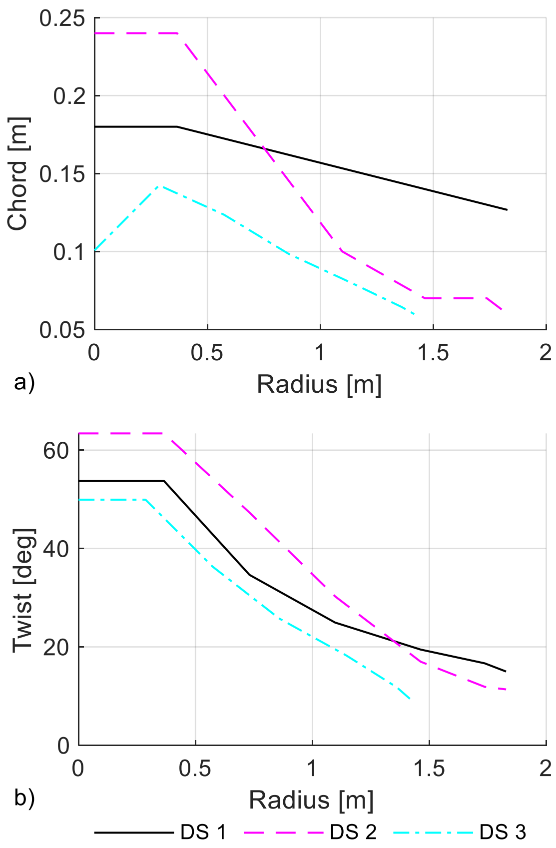

Figure 3 Chord (a) and twist (b) distribution of different design strategies

The assessment of the three DS shows the strength of DS 1 compared to DS 2 and DS 3 in the GPPO stage. The method is much faster and results in the best design point. DS 2 and 3 do not lead to the same Pareto front, so this DS should not be used in the GPPO stage.

To classify the results of the design strategies following example is made. The improvement of 0.7 kWs, which is equal to 770 Wh for the mission, could reduce the battery mass by approximately 3.9 kg, assuming an energy density of 200 Wh/kg [29]. This reduction in battery mass is a weight reduction in hover of 3.2 %, assuming that the design thrust in hover is equal to the aircraft mass.

4.2. Assessment of the Serial Optimisation Scheme

The design of the whole parameter space with GPPO and BSO is performed to assess the serial optimisation scheme. Subchapter 4.1 showed that the single optimisation of all parameters does not work. Therefore, it is not performed as a reference for this study.

Figure 4 shows the shift in the Pareto front from GPPO to BSO. Due to the serial approach, the Pareto front shifts towards lower sound pressure levels and energy consumption.

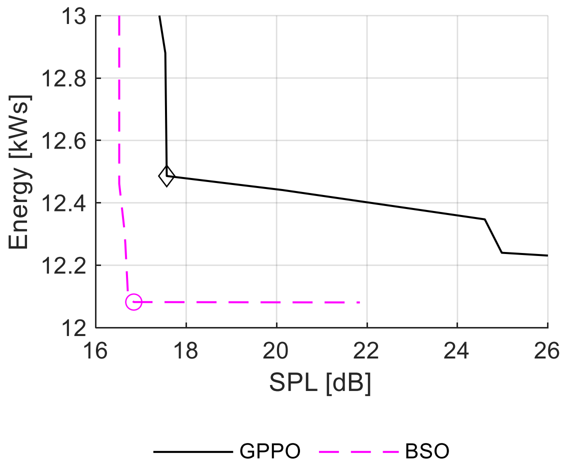

Figure 4 Blade shape Pareto fronts of the serial optimisation scheme

Table 5 summarises the results in the sweet spots of the GPPO and BSO. Within the GPPO, diameter and blade number are defined, and only twist and chord distribution are varied from GPPO to BSO. Sound pressure level and energy consumption are reduced due to the new blade geometry by 0.7 dB and 0.4 kWs. The serial approach requires about 11 hours of simulation time for optimisation.

Table 5 Optimisation sweet spots of GPPO and BSO

Design procedure		Serial	
		GPPO	BSO
Simulation time	[h]	2.5	8.2
Energy consumption	[kWs]	12.5	12.1
Sound pressure level	[dB]	17.5	16.8
Blades	[-]	8	8
Diameter	[m]	3.66	3.66

Finally, Figure 5 presents the chord and twist distribution. As required, the diameters are the same in both simulations. The twist distribution is nearly the same in both cases. The derivation from the GPPO stage to the BSO stage could be up to 30% in twist and chord distribution.

The chord distribution reduces from GPPO to BSO, leading to lower blade solidity.

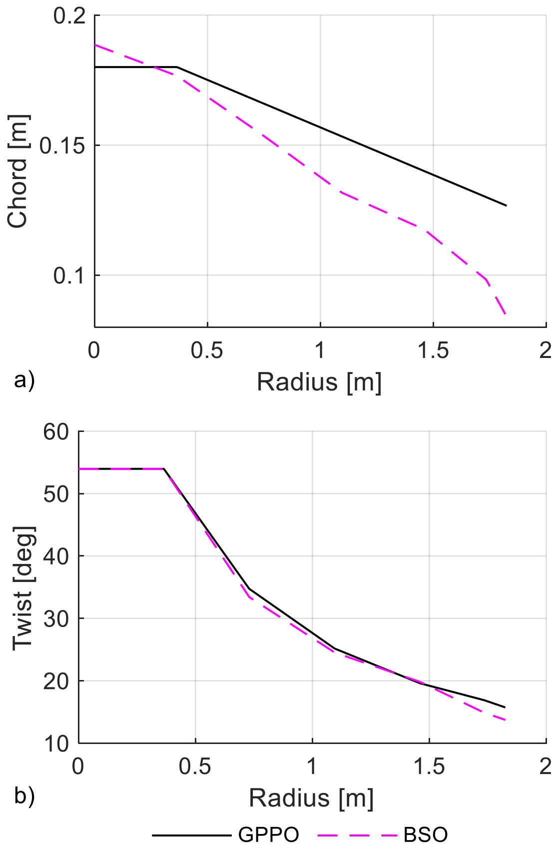

Figure 5 Chord (a) and twist (b) distribution of different optimisation schemes

The serial optimisation scheme improves the propeller's performance and noise emission. Compared to the GPPO stage with DS 3, the required time is similar, but the SPL is reduced by about 5 dB and the power consumption by 0.7 kWs. To achieve these results with DS 3 in a single step, the authors assume a simulation time of about five days to avoid local minima.

As in paragraph 4.1, the serial approach results are evaluated using the transformation of energy consumption to battery mass. The improvement of 0.4 kWs, which is equal to 440 Wh for the mission, could reduce the battery mass by approximately 2.2 kg, assuming an energy density of 200 Wh/kg [29]. This reduction in battery mass is a weight reduction in hover of 1.9 %, assuming that the design thrust in hover is equal to the aircraft mass.

5. CONCLUSION

This paper assesses different design strategies and optimisation schemes for multidisciplinary propeller optimisation. The propeller is optimised for a given flight mission encompassing multiple operating points and a single noise optimisation point. A novel serial optimisation scheme is presented. Within this optimisation scheme, three different propeller design strategies generate the geometries for optimisation.

The serial optimisation scheme reduces stepwise the parameter space. The first global propeller parameter optimisation defines the diameter and blade number. The blade shape optimisation is performed in the second step. At this stage, the twist and chord distribution are optimised. A propeller sweep optimisation can extend the design space.

One DS is required to define the propeller geometry in each optimisation step. The first propeller design strategy derives the MIL design, where only linear chord distributions are considered. A propeller is designed for a single operating point and analysed for the mission.

The second design strategy is an advanced MIL design algorithm capable of optimising a propeller for one operating point.

The third design strategy uses a polynomial description of the blade geometry.

The authors formulate two hypotheses for the optimisation procedure, which are analysed and confirmed within the paper.

1. A fast and robust design strategy should be used in the global propeller parameter optimisation, for example, DS 1. Higher complexity with larger optimization parameters tends to find local minima instead of global minima.
2. The serial optimisation scheme accelerates the design and improves performance and noise emissions.

The assessment of the optimisation scheme and propeller DS shows that a suitable approach can reduce the aircraft's weight by 5.1% using some basic assumptions.

In further work, the assessment of the acoustic models and the impact of the motor on the overall design should be evaluated. The acoustic model should also include a broadband noise model for higher accuracy in predicting noise emissions. Furthermore, minor variations of the diameter should be considered in the BSO. Diameter variation is not performed in this paper to reduce complexity.

Author contact:
Ole Bergmann: bergmann@fh-aachen.de

6. ACKNOWLEDGMENTS

The authors acknowledge the financial support by the Federal Ministry of Education and Research of Germany in the framework of IngenieurNachwuchs 2016 (project "DEFANA – Ducted Electric Fans for Novel Aircraft", project number 13FH638IX6) and the financial support of the FH Aachen University of Applied Sciences for funding the conference.

7. REFERENCES

[1] McKinsey & Company, "Study on the societal acceptance of Urban Air Mobility in Europe," McKinsey & Company, May. 2021.

[2] A. Betz and L. Prandtl, *Vier Abhandlungen zur Hydrodynamik und Aerodynamik*. Göttingen: Universitätsverlag Göttingen, 1919.

[3] C. N. Adkins and R. H. Liebeck, "Design of optimum propellers," in *Journal of Propulsion and Power 10*, 1994, pp. 676–682.

[4] E. E. Larrabee, "Design of propellers for motorsoarers," Massachusetts Institute of Technology, Massachusetts, 1979.

[5] E. E. Larrabee, "Practical Design of Minimum Induced Loss Propellers," MIT Massachuestts Institude of Technology, Cambridge MA, 1980.

[6] C. Dumont, L. Baert, and I. Lepot, "Multidisciplinary Design of a Low-Noise Propeller: Part I—Multi-Fidelity Design Methodology Leveraging on Acoustic Drivers," in *Turbo Expo: Power for Land, Sea, and Air*, 2020, V02DT38A022.

[7] O. Bergmann, F. Götten, C. Braun, and F. Janser, "Comparison and evaluation of blade element methods against RANS simulations and test data," in *CEAS Aeronautical Journal,* 13th ed., 2022, pp. 535–557.

[8] O. Bergmann, F. Möhren, C. Braun, and F. Janser, "On the influence of elasticity on swept propeller noise," in *AIAA SCITECH 2023 Forum*, National Harbor, MD & Online, 2023.

[9] F. Möhren, O. Bergmann, F. Janser, and C. Braun, "On the Influence of Elasticity on Propeller Performance: A Parametric Study," *Deutscher Luft- und Raumfahrtkongress 2021*, 2021.

[10] C. C. Hennes and K. S. Brentner, "The Effect of Blade Deformation on Rotorcraft Acoustics," in *31st European Rotorcraft Forum*, European Rotorcraft Forum, Ed., Florence, Italy, 2005, p. 398.

[11] F. Möhren, O. Bergmann, F. Janser, and C. Braun, "On the suitability of the Jig-Shape approach for structrual design of propellers," in *IFASD 2022*, International Forum on Aeroelasticity and Structural Dynamics, Ed., Madrid, Spain, 2022.

[12] O. Bergmann, F. Möhren, C. Braun, and F. Janser, "Aerodynamic Design of Swept Propeller with BEMT," in *DLRK 2022*, Deutsche Gesellschaft für Luft und Raumfahrt, Ed., Dresden, Germany, 2022.

[13] O. Gur and A. Rosen, "Multidisciplinary Design Optimization of a Quiet Propeller," *AIAA/CEAS Aeroacoustics Conference*, vol. 14, 2008-3073, p. 193, 2008, doi: 10.2514/6.2008-3073.

[14] D. B. Hanson, "Compressible Helicoidal Surface Theory for Propeller Aerodynamics and Noise," *AIAA Journal*, vol. 21, no. 6, pp. 881–889, 1983, doi: 10.2514/3.60132.

[15] F. Farassat, "Linear Acoustic Formulas for Calculation of Rotating Blade Noise," NASA Langley Research Center, Hampton, VA, 1980.

[16] B. Zaghari *et al.,* "The Impact of Electric Machine and Propeller Coupling Design on Electrified Aircraft Noise and Performance," in *AIAA SCITECH 2023 Forum*, National Harbor, MD & Online, 2023.

[17] O. Gur and J. Feldman, "Engine-Propeller Matching," in *The 62nd Israel Annual Conference on Aerospace Sciences*, IACAS, Ed., 2023. [Online]. Available: https://www.researchgate.net/profile/ohad-gur/publication/369362366_engine-propeller_matching/links/6416ced2315dfb4cce911ab5/engine-propeller-matching.pdf

[18] A. Kvurt, D. Ruf, O. Hertzman, O. Stalnov, and H. Ben-Gida, "getPROP - A MATLAB Suite for Low-Signature Propeller Design, Analysis, and Optimization," in *AIAA SCITECH 2023 Forum*, National Harbor, MD & Online, 2023.

[19] O. Gur and G. Lazar, "Prop-Rotor Design for an Electric Tilt-Rotor Vehicle," in *Future Vertical Lift Aurcraft Design Conference*, American Helicopter Society, Ed., Fisherman's Wharf, San Francisco, California, 2012.

[20] O. Bergmann, F. Möhren, C. Braun, and F. Janser, "Aerodynamic Analysis of Swept Propeller with BET and RANS," in *DLRK 2021*, Bremen, Germany, 2021.

[21] L. Gutin, "On the Sound field of a rotating propeller," *Physikalische Zeitschrift der Sowjetunion*, Band 9, Heft 1, 1936.

[22] O. Bergmann, F. Möhren, C. Braun, and F.

Janser, “Comparison of Various Aeroacoustic Propeller Noise Prediction Methodologies in Static Operations,” in *AIAA SciTech 2022 Forum*, San Diego CA, 2022.

[23] D. B. Hanson, “Helicoidal Surface Theory for Harmonic Noise of Propellers in the Far Field,” *AIAA Journal*, vol. 1980, no. 10, pp. 1213–1220, 1980, doi: 10.2514/3.50873.

[24] L. V. Lopes, “ANOPP2’s Farassat Formulations Internal Functional Modules (AFFIFMs) Reference Manual,” 20210021111, 2021.

[25] F. LECKIE and E. Pestel, “Transfer-Matrix Fundamentals,” *Int. J. Mech. Sci. Pergamon Press Ltd.*, vol. 2, pp. 137–167, 1960.

[26] O. Gur, “Airfoil Importance for Propeller Optimized Design,” in *56th 3AF International Conference of Applied Aerodynamics*.

[27] B. G. Marinus, M. Roger, and R. A. van den Braembussche, “Aeroacoustic and Aerodynamic Optimization of Aircraft Propeller Blades,” Royal Military Academy; von Karman Institute for Fluid Dynamics; Ecole Centrale de Lyon, Brussel, Belguim, Sint-Genesius-Rhode, Belguim, Ecully, France, 2010.

[28] N. S. Zawodny, N. A. Pettingill, L. V. Lopes, and D. J. Ingraham, “Experimental Validation of an Acoustically and Aerodynamically Optimized UAM Proprotor Part 1: Test Setup and Results: NASA/TM-20220015637,” Langley Research Center Hampton; Glenn Research Center Cleveland, Technical Memorandum 20220015637, Feb. 2023.

[29] O. Gur and A. Rosen, “Optimizing Electric Propulsion Systems for Unmanned Aerial Vehicles,” *Journal of Aircraft*, vol. 46, no. 4, pp. 1340–1353, 2009, doi: 10.2514/1.41027.